MJFAS MALAYSIAN JOURNAL OF FUNDAMENTAL AND APPLIED SCIENCES
PRINT ISSN: 2289-5981 | ONLINE ISSN: 2289-599X

RESEARCH ARTICLE

Review on a new austenitic 57Fe15Cr25Ni stainless steel at temperature of 850°C for 30 minutes followed by water quenching treatments

Parikin*, Mohammad Dani, Sulistioso Giat Sukaryo

Center for Science and Technology of Advanced Materials, BATAN Kawasan Puspiptek, Serpong Tangerang 15314, Indonesia

* *Corresponding author:* farihin@batan.go.id

Article History
Received 16 October 2018
Revised 29 November 2018
Accepted 3 February 2019
Published Online 15 October 2019

Abstract

Special steel demand is indispensable in nuclear field, especially as a construction material for structure of high temperature reactor. An austenite 57Fe15Cr25Ni stainless steel has been synthesized by using casting technique at temperature more than 1250°C in electromagnetic inductive-thermal furnace. The steel is comprised of (%wt) 57%Fe, 15%Cr, 25%Ni, 0.34%C and less than 0.1% of other elements: titanium, phosphor, copper, niobium and sulphur. Due to be promoted for a high pressure-temperature operating system, the material must has strength, creep and corrosion resistances. To increase the strength of the material, heat treatment is needed in certain cooling media, i.e. water. As suspected to temperature selection of 850°C, ferritic phase contributes to the strength of steel. The hardness of material increases up to 18% after being cooled rapidly into water medium. Even in the diffraction pattern, the ferritic phases do not grow clearly due to probably small amount of fraction. X-ray diffraction pattern shows that ascast with an fcc's lattice parameter of about 3.69 Å. Meanwhile, the water quenched sample has a lattice parameter which is slightly shorter than that ascast's lattice parameter, i.e. 3.59Å. The peak shift of the (111) plane in the profile diffraction, is shown approximately 0.079 degrees between ascast and water quenched samples, indicating the presence of residual strain that threatens the structural stability of the material. The ascast microstructure shows that austenite phase grains look very massive and illustrate irregular structures, with an average grain size of about 6-8 μm, showing coarse grains that are very different from the water quenched microstructure shown by fine grains and slightly porous. On the other hand, the viscosity (η) of quenching media has a very significant role in grain boundary formation (sensitization), because the rate of temperature drop is strongly influenced by heat diffusion from high to low temperature spaces at the surface of material. Moreover, there is no new phase formation and fatal scales in the corrosion appearance of the steel surface at 850°C after more than 15 hours of oxidation tests. Therefore, at temperature of 850°C, the steel is proven to withstand of its high temperature environmental corrosion.

Keywords: 57Fe15Cr25Ni austenitic steel, water-quenching, X-ray diffraction, electron-optical microscope, hardness, oxidation

INTRODUCTION

The development of structural material for nuclear reactors should be directed toward the high temperature resistance steels. This research activity had been proposed and initiated by the nuclear reactor material research group since 2006 at BATAN Indonesia. Laboratory scale fabrication of structural material candidates has been performed by the reactor material group using a casting method [1,2] by synthesizing the austenitic (A) and ferritic (F) series of super-alloy steel in order to yield the desired structural material with special advantages such as being able to withstand to creeps and corrosions.

Material engineers of BATAN proposed and synthesized an austenite steel type, which is non-standard composition with low carbon content, and might be dedicated to be applied as component of heat exchanger 'blade' materials which must have adequate high temperature corrosion resistance (oxidation). This austenitic stainless steel namely; A2 steel type which is synthesized from a mixture of raw local components. The steel is further called as 57Fe15Cr25Ni steel. The purpose of synthesizing the steels is to create a new type of steels with higher chromium-nickel content and significantly improved ductility and corrosion resistance properties of the materials.

In this research, the austenitic alloy steel containing (by %wt.): 57Fe, 15Cr, 25Ni, 0.34C and less than 0.1 of other elements including of titanium, phosphor, copper, niobium and sulphur is selected [2]. Some properties of austenitic steel have been characterized, i.e.: formability by mechanically cold rolled [3], weld-ability and residual stress measurements [4] in both treatments. The average hardness of the material is about 160 HVN (84HRC). The most current study reports that 57Fe15Cr25Ni steel shows a very excellent result in corrosion rate, which is almost 0.088 MPY [5].

Generally, stainless steel (SS) is made by adding at least 10% chromium (Cr) to iron. The SS then forms a chrome sesquioxide-based surface, oxide that sticks to the SS and prevents further corrosion [6]. This locks the material into the ferrite phase with body-centered cubic (BCC) structure. The material is strong enough and not

too brittle. Nickel (Ni) is often added to SS to convert the structure to the more ductile austenite phase and to add resistance to high temperature oxidation. One of the most common grades of SS contains 18% Cr and 8% Ni, usually produced in piping industry and household appliances like spoons and forks. In the US, this is known as type 303- or 304- SS. The austenitic steels generally contain 17-25% Cr with the content of others, namely by 8-20% Ni. In this austenite phase, the steel has the fcc (face centered cubic) unit cell. In the steady state, phase is determined at high temperatures. The solubility of carbon in austenite phase solubility must be greater than the solubility of the atoms in the ferrite phase (bcc; body centered cubic). Geometrically, solubility figures can be calculated by comparing the amount of space in the intensity of the austenite and ferrite phases.

Improving the mechanical properties of the materials can be engineered by giving heat treatments; by quenching techniques. Quenching [7] is a rapid temperature decreasing (cooling) process in which the temperature of the material is abruptly changed or heat dissipation from a metal at a certain speed which is at austenite temperature (815-870°C). This process is performed to increase the hardness, strength and toughness [8]. Quenching effects can alter crystal and micro-structures of the materials. The changes can properly be observed by diffraction techniques and microscopic analysis (Optical-Electron Microscopy).

In this article, the authors present a review on the performance of the 57Fe15Cr25Ni steel as a result of the heat treatments, i.e.: rapid cooling in water medium with comparative reference materials of ascast sample. This article covers a portion of extensive research work in oxidation resistance and micro-crystal structures due to heat treatments in which had been performed at temperature of 850°C for holding-time of 30 minutes.

MATERIALS AND METHODS

The working schema of research is completely listed in Fig. 1. 57Fe15Cr-25Ni austenitic steel was used in this work as experimental materials. The steel was fabricated by casting method which has been reported and discussed in the literature [2]. The alloying materials were melted in an induction furnace at temperature more than 1250 °C. This super austenitic alloy is a new austenite type of stainless steel that contained several alloying elements, such as chrome, nickel, manganese, silicon and carbon. Other elements, among them Ti was added in order to induce a relatively better pitting corrosion property due to reduced segregation [9,10,11]. Whereas: phosphor, copper, niobium and sulphur elements are other elements contained in the ascast as a prime material. The chemical composition in %wt of the materials is shown completely in Table 1. It was measured by a 1996 Swiss made Optical Emission Spectrometry (OES) in the Bandung Manufacture Polytechnique. The equipment was employed in elemental composition measurements by spark erosion method with a sample dimension of 2.5 x 2.5 x 12 cm3.

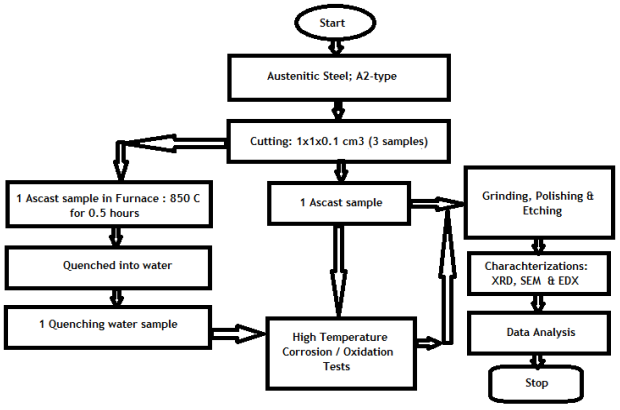

Fig. 1 Working chart of research.

Table 1 The chemical composition of 15Cr-25Ni austenitic alloy steel, resulted from spark errosion optical emission spectroscopy (OES).

Elemental Composition (%wt.)										
Fe	Cr	Ni	Si	C	Mn	Ti	S	P	Cu	Nb
57.74	15.42	25.01	0.96	0.34	0.32	Impurity ≤ 0.1				

The ascast materials were cut into 2 parts by using a diamond wafering blade to a dimension of 1x1x0.1 cm^3. One of the samples was heat-treated in the furnace with a rate of about 11°C/minute until reached temperature of 850°C for 30 minutes. The temperature selection of 850°C was expected to increase the strength of the material, especially the hardness, where of Fe-C diagram at this temperature showed that the ferritic phase was began to form at the grain boundaries. It was rapid quenched into cooling medium of water to trap the phases. The 850°C quenched sample was then consequently labelled as water quenching sample, whereas ascast was as a reference sample. Several steps of metal preparation process including: cutting, grinding, polishing and finished by pasta and ethanol–cleaning were conducted, until the samples surface became smooth and shiny with no scratch left.

Furthermore, the crystalline space group of both samples was verified by collecting reflection intensities using an X-ray diffractometer. Cu-target of wavelength (λ=1.54 Å) was utilized in measurements by the PANalytical Empyrean diffractometer machine in BATAN. The samples were run and scanned in the 2θ-range of 40 to 100 degrees with step counting of 0.02 degree and preset count mode of 2 second.

The samples were then chemical-etched by the Kalling's reagent (HCl and CuCl2) solution to clean the entire surface of the sample from undesirable impurities. After going through the process of etching, surface of the test sample became opaque (dop). Then, the sample was inspected by using both optical (OM) and electron (SEM) microscopes. Grains and grain boundaries shown might be depictioned between point to point views, searching the disclosure differences. The microstructures investigation was carried out by a standard procedure [12,13]. The characterization was accomplished by using an Olympus- Optical Microscope and a JEOL-Electron Microscope (SEM). SEM images were recorded by using secondary electron detector (SEI) at the acceleration energy of the primary electron beam source tungsten wire by a maximum of 20 keV with a working distance (WD) kept constant at 10 mm. WD value was setup to get EDX spectrum in the best condition. EDX was taken on the value of dead time on average between 20% and 40%. More detailed information has been discussed in previous publications [12].

Moreover, high-temperature-corrosion (oxidation) tests were conducted on the samples both on the ascast and the water-quenched samples. Both types of austenitic steel samples were initially weighed using analytical balance and then tested for oxidations by heating in a Scientific furnace at 850°C for more than 15 hours [14]. Samples were weighed again, at a periodic interval of more than 5 hours, to determine the weight gain due to corrosion. The sample's surface was then treated according to the preparation process outlined in the working chart of Fig. 1. Measurements with other methods could also be carried out by using the Magnetic Suspension Balance (MSB) [15]. Firstly, six same-size segments of A2 type austenitic steel, each with a dimension of (1.0 x 1.0 x 0.1 cm3) was cut from a single bar. Three segments from each of both the ascast sample and the quenched sample. The ascast sample was a preliminary sample that was given no heat treatment while the quenched sample was a preliminary sample that has been heated using a blast furnace at 850°C for 30 minutes and then rapidly dipped into water.

RESULTS AND DISCUSSION

Crystal structure

Fig. 2 shows the X-ray diffractogram for 57Fe15Cr25Ni steel obtained by using PANalytical Empyrean. Five characteristic peaks corresponding to the (111), (200), (220), (311) and (222) diffraction planes appeared conspicuously above the background counts at the

consecutive 2θ-diffraction angles at 43.5°, 51°, 75°, 91° and 96.5°. The Miller indices are grouped as all odds or all evens which are typical for a face centered cubic (fcc) space group. The observed counting intensity of the water quenched sample was lower than the intensity counts of the ascast sample at plane (111). So, the pattern of the water quenching sample was broader than ascast sample. Probably, this can predict that the crystallite size in the ascast sample is greater than of the water quenched sample.

The ascast sample showed a very sharp peak, even the second wavelength ($K\alpha_2$) was appeared in every primary peaks. In this case, if the surface area and X-ray irradiation time on the material are same, then the integrated intensity (area under the peak) of low broaden peaks (water-quenched) and high sharp peaks (ascast) should be equal or the same. Consequently, the crystallite sizes corresponding to the low broaden peak were smaller than those corresponding to the high sharp peaks. Rapid cooling process may foster the crystallite size or grains of the materials due to crystallite sizes that are relatively very large while peak intensities are sharp and high. The process of quenching steel into a water medium can decrease the size of the crystallite material. With a possible phenomenon, in which, when the material is heated, crystallites move through the grain boundaries and rearrange themselves to form larger colonies while they will be fragmented when experiencing a momentary cooling. In a homogeneous state, the material is then dipped rapidly into the water with an extreme temperature difference, such that the material granules do not return back into the original shape, such as ascast conditions. Also, there was no filter for $K\alpha_2$ in the X-ray diffraction system that contributed to the pattern as second peak inside the principal peak (see Fig. 3).

The quench treatment in different media influences the dynamics of the crystal lattice. It is widely observed in the steel samples that crystal lattice tends to execute the 'stretch and shift' modification around the 2θ reflection angle. Peak position may shift to the left and right. It can be seen in Fig. 3 that, if ascast profile considered as the origin, water-quenched sample profile would move to the left from the starting profile for about of 0.079 degrees. Table 2 lists the parameters of the refinements of the profiles, supporting the shifting phenomenon (Δ2θ). Refinement results of X-ray diffraction pattern showed that ascast material has an *fcc* unit cell with lattice parameter of 3.69 Å. Meanwhile, water quenched samples has a lattice parameter slightly lower than ascast's lattice parameter, i.e. 3.59 Å.

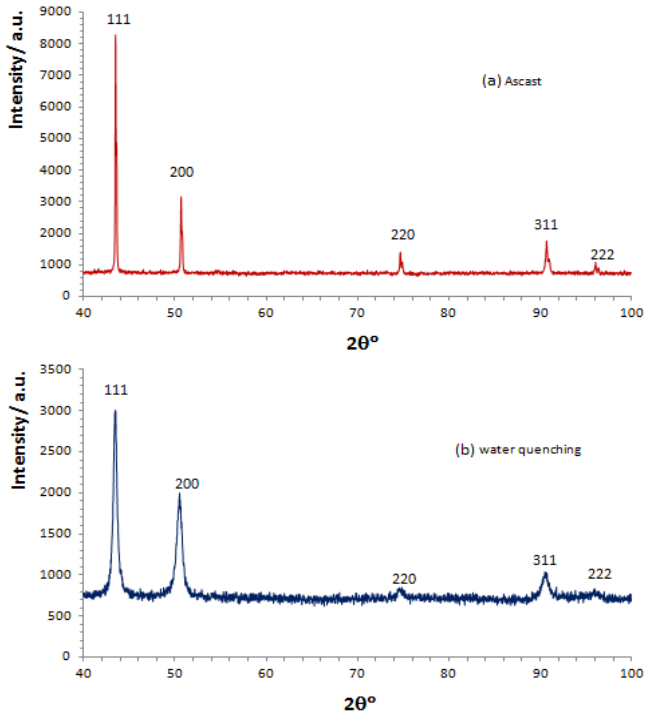

Fig. 2 X-ray diffraction patterns of 57Fe15Cr25Ni steel sample (a) ascast and (b) quenching of temperature 850°C to water.

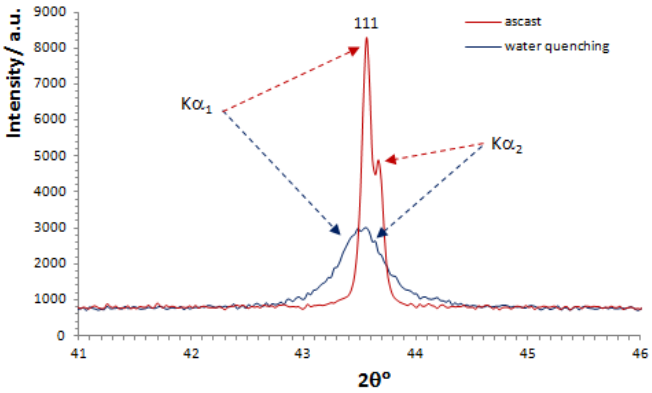

Fig. 3 Shifting and broadening peak of 57Fe15Cr25Ni steel sample for (111) plane, indicating the presence of residual strain-stresses in the steel.

Table 2 Refinement parameters of the profiles at (111) reflection.

Sample	*a* (Å)	2θ (°)	Δ2θ (°)	fwhm (°)	R_{wp}	S
Ascast*	3.69	43.632	-	0.0801	4.36	1.35
Water quenching	3.59	43.553	-0.079	0.3887	4.70	1.42

The peak shift of (111) plane in the profile diffraction was very significant, in which approximately 0.08 degrees between ascast and water quenched samples. The shifting can further affect the stretching of crystal lattice, causing in the residual tension-compression in the material. This indicates the presence of residual strain-stress that threatens the structural stability of the material. Fig. 3 clearly shows the angular 2θ peak shifted from the sequence of ascast and water quenched samples, observed from (111) plane. The water quenching may cause a residual tension in the sample, due to the occurrence of shift-distance of about 0.079°. This sample may hardly be attacked by the corrosion that threatens the structural stability of the material. As a consequence, the water quenched sample would corrode faster than the ascast samples and face early fragility. However, phase analysis (see in Fig. 2) with X-ray diffraction clearly displayed no identifiable phase corrosion products.

Microstructure

The morphologies of the products were observed using the SEM measurements taken on the SEM-JEOL instrument. Fig. 4 shows the SEM images of the (a) ascast and (b) water quenched samples of the steel, with a magnifcation of 1.500x. The diameter of the ascast sample′s globular grains was found to be 6-8 μm [14,16]. Also, it is shown in Fig. 4(a) that the precipitates (black spots) were distributed along the grain boundaries and some were trapped inside the grains of the surface. In Fig. 4(b), the grains swollen after samples were water-quenched from temperatures of 850°C. The matrix grains undergo rearrangement in which small grains join together to form large colonies. Grains orientation is apparently still led to the (111) and (200) planes. Furthermore, the diffraction pattern of ascast showed a very high intensity in both the (111) and the (200) reflections as a consequence of the grains′ enlargement.

It is very apparent in Fig. 4b that black oval-porosities were still presented in the sample surface and smaller precipitates were spread evenly throughout the surface of the water-quenched sample, comparing to the ascast sample (Fig. 4a). There is a sufficient reason to believe that at 850°C, the precipitates are not concentrated enough in the grain boundaries but they are expected to move freely throughout the material surface, resulting in the fixed arrangement of precipitates in the last position where they are located when the sample is exposed to an abrupt rapid cooling process. As a result, dislocation movement in the material can be blocked, leading to an increase in hardness of the material.

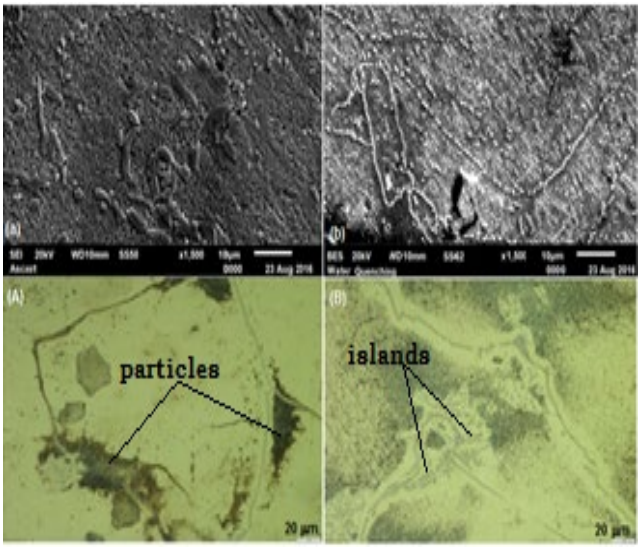

Fig. 4. Electron Microscope (SEM; 10µm) of (a) ascast and (b) 850°C-30 minutes of water quenching samples; with magnification of 1500x. Respectively, Optical Microscope (OM-20µm) of (A) ascast and (B) 850°C-30 minutes of water quenching samples; with magnification of 500x to show islands (elongated fractures) and particles (black spots) in grains and grain boundaries.

Due to the differences in viscosity [17] of the quenching medium (which is $\eta_a<\eta_w$), the decrease of temperature in water medium is successively faster than in air medium. So, the process of forming grains in water medium looks more refine than in medium of air. Otherwise, the fluid homogeneity may cause different effect; air can strike or damage an increasing segment of a sample's surface, while water favours to erode the grain boundaries (such as irrigation basins). Meanwhile, the surface micrograms of the ascast and the quenched samples after heating have shown no occurrence of significant phase changes. Electron microscope (SEM) showed no damage on the material surfaces due to quenching process, except for the changes in grain size.

Furthermore, in order to gain information on the impact test, microstructural scenes of the materials obtained were not much different from Fig. 4, which can be seen and enlarged in Fig. 5 and 6. Fig. 5 shows the surface microstructures of the ascast sample which scaled of 25 micron for a close-up of material surface around the boundary. It was found that the porosity trapped in grain lines was surrounded by a very high concentration of Cr colonies. In addition, Cr elements were concentrated in the grain boundaries as corresponded to EDX spectrums in Fig. 5. Cr quantity presented almost of about 63.36% wt. in boundary (5a) and 17.45 %wt in matrix (5b). EDX spectrums [18] in Fig. 5b also shows that the carbon (C) elements did not occupy the sites in the steel's matrix. The elements were concentrated at the grain boundaries, more precisely in the coagulated precipitation that formed at the grain boundaries (which has the lowest energy). Meanwhile, Si (1.33 %wt.) and Ni (26.11 %wt.) elements were detected to occupy the surface of steel matrix. Otherwise, there was a lack of Ni (4.62 %wt.) at the grain boundaries. Some coagulations (precipitate growths) form clusters in a series of circular boundary lengths, encircling the steel matrix. So the line boudaries look thickened if it is obseved by a small magnification scale of the lens. It seems that the carbon elements apparently prefer to react with the Cr elements to form carbide compounds. Usually the compounds are derivation of $Cr_{23}C_6$. Another study has confirmed that the effects of $Cr_{23}C_6$ compound may reduce the toughness of the materials due to initiation of the cracks' formation [19].

Fig. 6 shows a physical change in the precipitate microstructures due to the rapid cooling process from 850°C to the temperature of the water environment. SEM micrograph reveals that there was a form of precipitate shift that originally spread irregularly into the boundary, as if it was dissolved into a small spherical shape with a thin and long stretch of grain boundary mesh. From the analysis of the energy dispersive spectrum (EDX), it was shown that Fe-Cr-Ni content dominated the ascast sample while in the water quenched sample, the content of (Fe;Cr) elements was very high and they were apparently the main instigator of precipitates compounds formation. Fe and Cr contents were counted sequentially reaching quantity of 28.56 and 51.82% wt. If the elements meet the carbon element, they are hypothesized to form precipitates Fe3C or Cr23C6 [20] along the grain boundaries. These precipitates should be eliminated, since they can generally wrap the material and reduce the toughness of the materials.

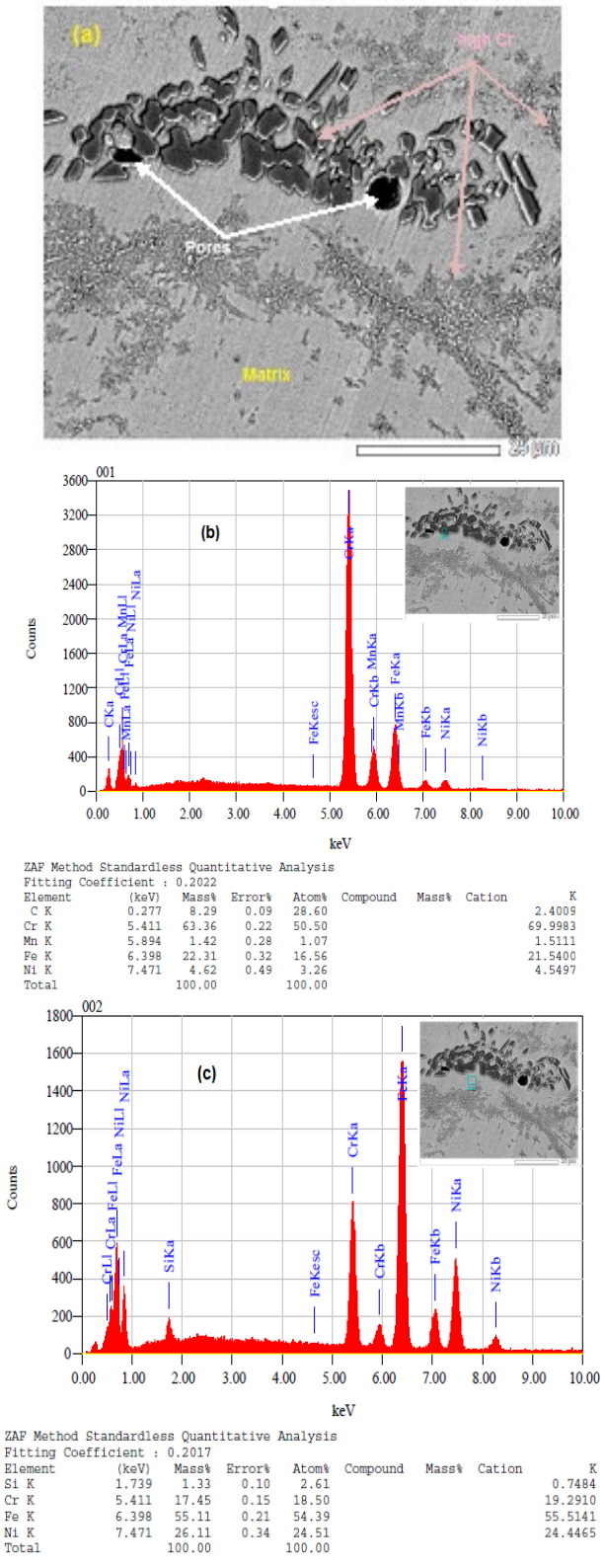

Fig. 5 (a) SEM micrograph (25µm) of ascast sample and EDX spectrums on (b) precipitate and (c) matrix positions.

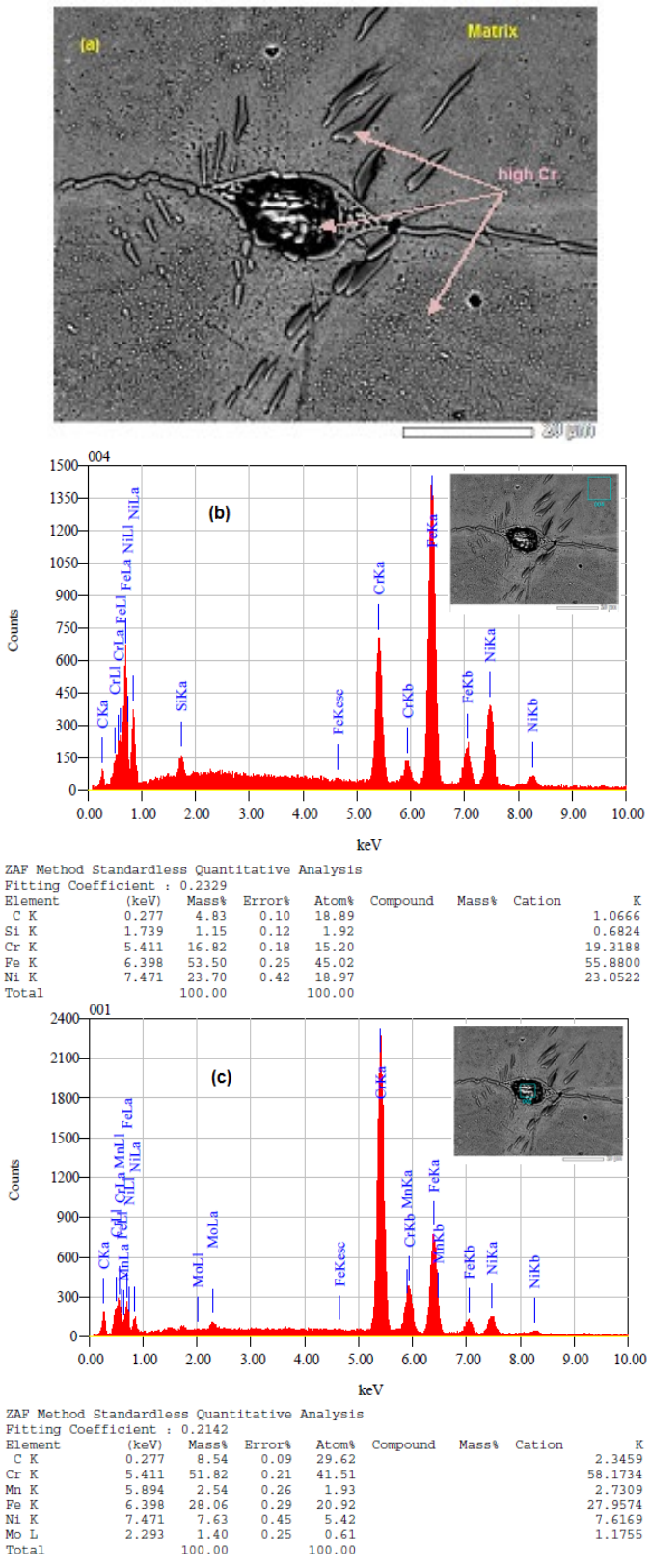

Fig. 6 (a) SEM micrograph (20µm) of water-quenching sample and EDX spectrums on (b) matrix and (c) grain boundary (on precipitate).

Hardness

Quenching treatment is one of the methods to increase the hardness of metals. As expected to that of temperature selection of 850ºC, ferritic phase would contribute to strength of the steel. Hardness was increased after the steel being cooled rapidly into water medium. Even in the diffraction pattern, the peaks of ferritic phase did not grow clearly due to probably their small amount fraction. Fig. 7 shows the results of austenitic 57Fe15Cr25Ni steel surface hardness measurements by Vickers method. After quenching to water medium under normal environmental conditions, hardness of 57Fe15Cr25Ni steel has increased by almost 18% from 163.33 kg/mm2 to 193.33 kg/mm2. Increasing the hardness of this material is possible to be occurred by precipitation hardening where it tends to be diffused toward and concentrated in the grain boundaries. Increased hardness on the surface is needed and is an advantage, in order for the material to be more wear resistant and ductile, so that, the toughness of the material can be guaranteed to be safe in every application. Increased hardness on the surface of the material can be utilized to increase the strength of the material to be more resistant to fungal-triggered corrosion (freeting corrosion), where this corrosion is one of the prime causes of the metal scales.

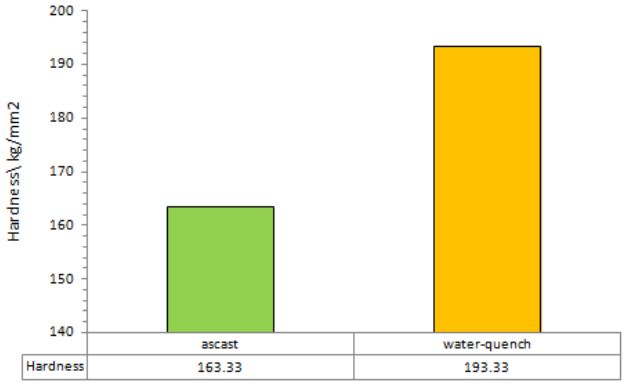

Fig. 7 Hardness of 57Fe15Cr25Ni steel sample (a) ascast and (b) quenching of 850ºC to water.

High temperature corrosion resistance

The measurement of oxidation resistance [21] curve of the steel samples was based on the increase of weight gain obtained from the sample heating for more than 5 hours. The weight gain of each sample was estimated using an analytical balance. For each group of the sample (3 pieces), the experiment was performed for almost more than 15 hours (20000 seconds for each sample), as shown in Fig. 8. The curve showed the change in the weight gain of the heating time of the quenching and ascast samples weighed by the balance. The results showed that the weight gain of the quenching sample was greater than the ascast sample with the rates of 0.0802 mpy and 0.06 mpy, respectively. This is very suitable when comparing with F1-type ferritic steel [5], where the corrosion rate of this steel looks almost the same as the corrosion rate of steel 'water-quenching' sample. Also, it is very different from AISI 430 commercial steel which has a lower corrosion resistance rate of only 0.1142 mpy [5]. The weight gain is fully influenced by the oxide that formed after the sample material is being heated, so it can be assumed that the ascast sample is more oxidant-resistant than the quenching sample.

As a result, Fig. 9 shows the cross-section microstructures of surface sample from the oxidation test. The images displayed more scales at surface of the quenching sample after oxidation at temperature of 850°C for 15 hours (9b) than ascast sample with the same condition. These morphological photographs showed enough surface scale due to oxidation. The ascast sample's surface in Fig. 9a was smooth. The shaft boundary was intact or no-corrosion scales, while the surface of the quenched sample (9b) was clearly visible due to corrosion scales, where fragility and material fragments (corrodants) were distributed around the porosity position. Corrodant colonies were seen as oxidized areas. The areas looked brighter in color than the surrounding areas (see Fig. 9b). It is also possible that the scales are due to interaction with other elements when being heated especially with oxygen elements (see the curve for water quenching sample has higher rate than the ascast one). In addition to the above microstructure information where ascast has a pattern of precipitation that spreads throughout the surface of the material, which makes the defense of corrosion attacks more resistant than water quenching samples which have a centralized precipitation pattern like a ball along the grain boundaries.

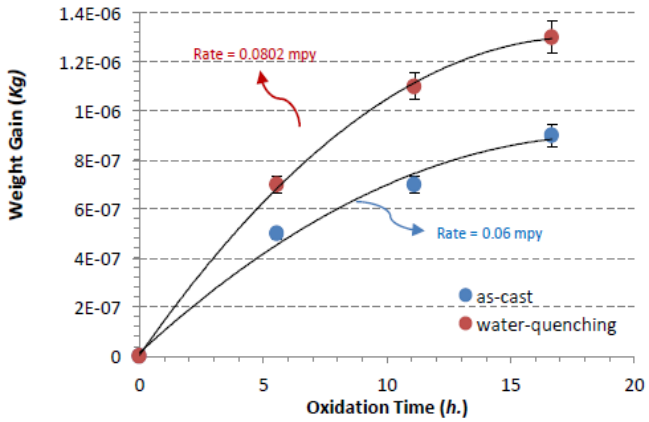

Fig. 8 Additional weights in ascast and water-quenching samples versus oxidation time [14].

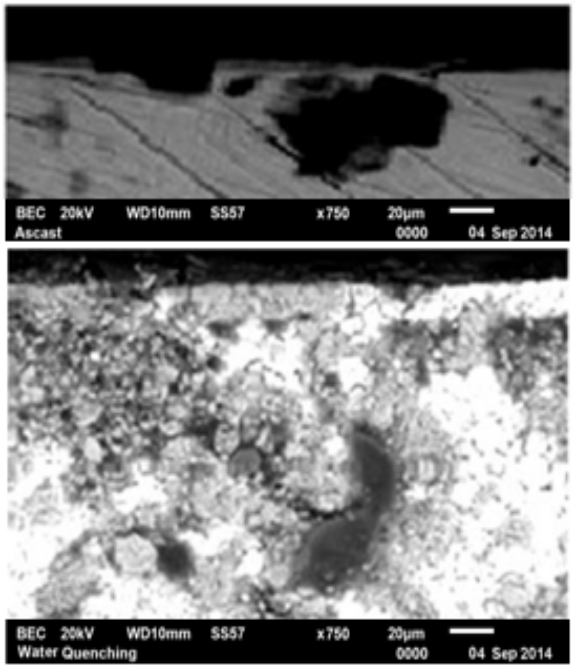

Fig. 9 Cross-section microstructures [14] of the 57Fe15Cr25Ni austenitic steel taken by SEM-JEOL (20 µm); (a) ascast and (b) water-quenching sample.

Table 3 EDX counting [14] for the elemental corrosion products (%wt.).

Elements (%wt.)	Fe	Cr	Ni	Si	Mn	C	O
Ascast	53.90	15.50	11.95	1.22	0.31	14.65	2.00
Water quenching	48.79	19.08	5.53	0.89	2.10	26.69	16.94

Semi-quantitative analysis of the elements in the samples by using SEM-EDX [14], supported the phenomenon of weight gain above. Some of the major constituents of the material and oxygen elements as key information on the oxidation events were clearly detected, as arranged in Table 3. In both samples, the O element was detected with the amounts of 2.0 %wt. and 16.94 %wt. for ascast and water-quenching samples, respectively. There is an interesting phenomenon when the data is being compared, in which the oxygen element content in the quenching sample is larger than the ascast sample, but the difference is less significant. This contradiction indicates that ascast sample does not mean to be more resistant to high temperature corrosion compared to quenching sample. A possible statement for this phenomenon is the significant role of the ability of Cr element to form a passive layer (Cr_2O_3) on a very large surface material by binding O element. Also, the high Ni content is capable of forming spinels that can inhibit the movement of element O on surface of the material. So the material is able to cope with a very small oxidation product.

CONCLUSION

As expected to that of temperature selection of 850°C, the ferritic phases could contribute to the strength of steel. The hardness of material was increased up to 18% after being cooled rapidly into water medium. Even, in the diffraction pattern, the ferritic phases did not grow clearly due to probably small amount fraction. X-ray diffraction pattern showed ascast sample with an fcc's lattice parameter of about 3.69 Å. Meanwhile, the water quenched sample has a lattice parameter which was slightly shorter than ascast's lattice parameter, i.e. 3.59Å. The peak shifts of the (111) plane in the profile diffraction was shown approximately of 0.079 degrees between ascast and the water quenched samples, indicating the presence of residual strain that threatens the structural stability of the material. Ascast microstructure revealed that the austenite phase grains looked massive and described an undeformed structure, with an average grain size of about 6-8 µm, showing a coarse grain which was very different from the water quenched microstructure shown by fine grains and little bit porous. On the other hand, the viscosity (η) of the quenching medium has an important role in the formation of grain boundary (sensitization), because the rate of decreasing temperature is heavily influenced by the heat diffusion from the high to low temperature space in the surface materials. Moreover, there was no new phase formation and fatal scales in the corrosion products of the 57Fe15Cr-25Ni steel at 850°C after more than 16 hours of oxidation tests. Therefore, at temperature of 850°C, the steel was proven to withstand its high temperature environmental corrosion.

ACKNOWLEDGEMENT

The authors would like to express their thanks to head of PSTBM and BSBM. The authors were grateful to Mr. Sumaryo, Mr. Rohmad Salam, Mr. Joshua E. Gunawan, Miss. Ambar and Mr. Agus Sujatno, who have been taking parts in this research. Also, authors would like to specially thank to all official mates for their kindness and helps. Financial supports from DIPA Program year of 2016 in R&D of PSTBM-BATAN were acknowledged.

REFERENCES

[1] A. E. W. Jarfors. (2016). Casting alloy design and modification, *Metals*, 6(15), 1-2.

[2] N. Effendi, A. K. Jahja, Bandriana, W. A. Adi. (2012). Some data of second sequence non standard austentic ingot A2-Type, urania, *Scientific Journal of Nuclear Fuel Cycle*, 18(1), 48-58.

[3] Parikin, N. Effendi, H. Mugihardjo, A. H. Ismoyo. (2014). Studi pengaruh rol panas pada tegangan sisa bahan struktur baja A-2 non standar dengan teknik difraksi neutron, urania, *Scientific Journal of Nuclear Fuel Cycle, 20*(1), 33-42.

[4] Parikin, A. H. Ismoyo, R. Iskandar, A. Dimyati. (2017). Residual stress measurements on the TIG-Weldjoint of 57Fe15Cr25Ni austenitic steel for structure material applications by means X-Ray diffraction techniques, *Makara Journal of Technology*, University of Indonesia *21*(2), 49-57.

[5] I. Wahyono, R. Salam, A. Dimyati, Parikin. (2015). Karakterisasi struktur mikro menggunakan SEM dan XRD pada ketahanan korosi baja komersial SS430 dan baja non komersial F1, *Prosiding Seminar Nasional SDM Teknik Nuklir Yogyakarta*, 15 September, Yogjakarta, 112 – 117.

[6] Y. Shi, B. Yang, P. K. Liaw. (2017). Corrosion-resistant high-entropy alloys: A review, *Metals 7*(43), 1-18.

[7] S. Y. P. Allain, G. Geandier, J.-C. Hell, M. Soler, F. Danoix, M. Gouné. (2017). Effects of Q&P processing conditions on austenite carbon enrichment studied by in situ high-energy X-ray diffraction experiments, *Metals 7*(232), 1-13.

[8] M. Tocci, A. Pola , L. Montesano , M. Merlin , G. L. Garagnani, G. M. L. Vecchia. (2017). Tensile behavior and impact toughness of an AlSi3MgCr alloy, *Procedia Structural Integrity 3*, 517–525.

[9] Y. Hu, Y. H. Shi, X.Q. Shen, Z.-M. Wang. (2017). Microstructure, pitting corrosion resistance and impact toughness of duplex stainless steel underwater dry hyperbaric flux-cored arc welds, *Materials 10*(1443), 1-18.

[10] A. K. Singh, G. M. Reddy, K. Srinivas Rao. (2015). Pitting corrosion resistance and bond strength of stainlesssteel overlay by friction surfacing on high strength low alloy steel, *Defence Technology 11*(3), 299-307.

[11] R. T. Loto. (2015). Pitting corrosion evaluation and inhibition of stainless steels: A review, *Journal of Materials and Environmental Science 6*(10), 2750-2762.

[12] A. Sujatno, R. Salam, B. Bandriyana, A. Dimyati. (2015). Studi scanning electron microscopy (SEM) untuk karakterisasi proses oxidasi paduan zirkonium, Jurnal Forum Nuklir (JFN), 9(2), 44-50.

[13] M. Dani, Parikin, A. K. Jahja, A. Dimyati, R. Iskandar, J. Mayer. (2017). Investigation on precipitations and defects of the Fe-24Cr-2Si-0.8Mn ferritic super alloy steel, *Jusami (Indonesia Science and Materials Journals) 18*(4), 173-178.

[14] Parikin, B. Sugeng, M. Dani, S. G. Sukaryo. (2017). Ketahanan korosi temperatur tinggi baja super austenit 15% Cr-25% Ni pada temperatur 850ºC, *Jurnal Sains Materi Indonesia (Indonesia Materials Science Journal) 18*(4), 179-184. in Indonesia

[15] R. Salam, Bandriyana, A. Dimyati. (2013). Uji fungsi magnetic suspension balance (MSB) untuk penelitian material temperatur tinggi, *Prosiding Seminar Nasional SDM Teknik Nuklir Yogyakarta*, 242-246.

[16] Parikin,T. H. Priyanto, A. H. Ismoyo, M. Dani. (2015). Hot-rolling effects on mechanical properties of 15%Cr-25%Ni steel plates for reactor structure materials, *Jurnal Sains Materi Indonesia (Jusami) 17*(1), 22-28.

[17] D. Kim, S. Hong, J. Jang, J. Park. (2017). Determination of fluid density and viscosity by analyzing flexural wave propagations on the vibrating micro-cantilever, *Sensors 7*(11), 2466-2475.

[18] T. L. Burnett, R. Kelley, B. Winiarski, L. Contreras, M. Daly A. Gholinia M. G. Burke, and P. J. Withers. (2016). Large volume serial section tomography by Xe plasma FIB dual beam microscopy, *Ultramicroscopy,* 161, 119–129.

[19] Parikin, M. Dani, A. K. Jahja, R. Iskandar, J. Mayer. (2018). Crystal structure ivestigation of ferritic 73Fe24Cr2Si0.8Mn0.1Ni steel for multipurpouse structural material applications, *International Journal of Technology 9*(1), 78-88.

[20] N. Effendi, T. Darwinto, A. H. Ismoyo, Parikin. (2014). 24-chromium ferritic steel magnetic properties, Jurnal Sains Materi Indonesia *Indonesia Materials Science Journal 15*(4), 187-190.

[21] J. Metsäjoki, M. Oksa, S. Tuurna, J. Lagerbom, J. Virta, S. Y. Olli, T. Suhonen. (2015). Tailoring a high temperature corrosion resistant FeNiCrAl for oxy-combustion application by thermal spray coating and HIP, *Coatings 5*, 709-723.